



## Assessing spatial variability of extreme hot weather conditions in Hong Kong: A land use regression approach



Yuan Shi<sup>a,\*</sup>, Chao Ren<sup>a,b,c</sup>, Meng Cai<sup>a</sup>, Kevin Ka-Lun Lau<sup>b,c,d</sup>, Tsz-Cheung Lee<sup>e</sup>, Wai-Kin Wong<sup>e</sup>

<sup>a</sup> School of Architecture, The Chinese University of Hong Kong, Shatin, NT, Hong Kong, China

<sup>b</sup> The Institute of Environment, Energy and Sustainability (IEES), The Chinese University of Hong Kong, Shatin, NT, Hong Kong, China

<sup>c</sup> Institute Of Future Cities (IOFC), The Chinese University of Hong Kong, Shatin, NT, Hong Kong, China

<sup>d</sup> CUHK Jockey Club Institute of Ageing, The Chinese University of Hong Kong, Shatin, NT, Hong Kong, China

<sup>e</sup> Hong Kong Observatory, Kowloon, Hong Kong, China

### ARTICLE INFO

#### Keywords:

Extreme hot weather events  
Land use regression  
Spatial mapping  
Land surface morphology  
Hong Kong

### ABSTRACT

The number of extreme hot weather events have considerably increased in Hong Kong in the recent decades. The complex urban context of Hong Kong leads to a significant intra-urban spatial variability in climate. Under such circumstance, a spatial understanding of extreme hot weather condition is urgently needed for heat risk prevention and public health actions. In this study, the extreme hot weather events of Hong Kong were quantified and measured using two indicators – very hot day hours (VHDHs) and hot night hours (HNHs) which were counted based on the summertime hourly-resolved air temperature data from a total of 40 weather stations (WSs) from 2011 to 2015. Using the VHDHs and HNHs at the locations of the 40 WSs as the outcome variables, land use regression (LUR) models are developed to achieve a spatial understanding of the extreme hot weather conditions in Hong Kong. Land surface morphology was quantified as the predictor variables in LUR modelling. A total of 167 predictor variables were considered in the model development process based on a stepwise multiple linear regression (MLR). The performance of resultant LUR models was evaluated via cross validation. VHDHs and HNHs were mapped at the community level for Hong Kong. The mapping results illustrate a significant spatial variation in the extreme hot weather conditions of Hong Kong in both the daytime and nighttime, which indicates that the spatial variation of land use configurations must be considered in the risk assessment and corresponding public health management associated with the extreme hot weather.

### 1. Introduction

Climate change has become a major challenge to human health and environmental sustainability (WMO, and WHO et al., 2015; IPCC, 2014). It has been foreseen that not only a warming trend is ahead, but also extreme hot weather events would become more intense, more frequent, and longer lasting (Meehl and Tebaldi, 2004; Field, 2012; Stocker, 2014). Under such circumstance, heat-related health impact has become an increasing concern for environmental health (Hajat and Kosatsky, 2010). With more than half of the global population now living in cities, the United Nations adopted the New Urban Agenda in 2016 to set a new global standard and roadmap for sustainable urban development, including the actions to address climate change and strengthen the resilience of cities for reducing the risk and impact of natural disasters (UN, 2016). In this regard, urbanized areas are of emerging concern because the urban heat island (UHI) effect further exacerbates the intensity and frequency of the heat wave and extreme

hot weather events (Oke, 1973; Oke, 1997; Tan et al., 2010; Li and Bou-Zeid, 2013). Such situation makes cities, especially high-density and compact large cities more vulnerable to extreme hot weather (Uejio et al., 2011; WMO and WHO et al., 2015).

Urban climatic condition varies at different locations within the city due to the spatial differences in land use configurations and inhomogeneous land surface characteristics (Hart and Sailor, 2009). This leads to a significant spatial variability in the extreme hot weather condition. For example, an urbanized area with dense building clusters absorbs more shortwave solar radiation during the daytime and releases more longwave radiation during the nighttime. The deep street canyons in urban areas trap the heat and consequently accumulate more heat than rural areas (Arnfield, 2003). There are also other effects from the spatially varied urban wind environment (Comrie, 2000) and anthropogenic heat (Taha, 1997). As the results, urban areas would experience more prolonged and intense heat wave events than rural areas under similar background meteorological condition. Moreover, the intra-

\* Correspondence to: School of Architecture, The Chinese University of Hong Kong, Rm505, AIT Building, Shatin, NT, Hong Kong, China.  
E-mail address: [shiyuan@cuhk.edu.hk](mailto:shiyuan@cuhk.edu.hk) (Y. Shi).

urban spatial variation in urban configuration/building environments also leads to the intra-urban differences in the frequency, intensity, and duration of the heat wave events. It has been indicated that people living in intra-urban areas experience a more intense UHI (Clarke, 1972) and consequently at a higher heat-related life risk (Besancenot, 2002). However, many of current studies on the heat waves or extreme hot weather events prediction, heat-related urban vulnerability and health impacts are based solely on the temporal analysis, but lack of a more comprehensive spatial understanding (Kaiser et al., 2007; Le Tertre et al., 2006; Kysely, 2002). In such cases, the evaluation of urban vulnerability to extreme hot weather and the prevention strategies-making would be biased due to “The Uncertain Geographic Context Problem (UGCoP)” (Kwan, 2012). Kwan (2012) points out that the findings on the influence of area-based attributes on the outcomes of individual could be affected by the geographic delineation of contextual units or neighbourhoods because of the spatial uncertainty. The effects of UGCoP are even more significant in large cities with a complex geographic context. Therefore, acquiring a detailed spatial understanding of the extreme hot weather events is essential to heat risk prevention and public health actions (Buscail et al., 2012). In recent years, relevant studies have been conducted for the spatial mapping of heat-related risks in many large or megacities worldwide (Klein Rosenthal et al., 2014; Wolf and McGregor, 2013; Lemonsu et al., 2015; El-Zein and Tonmoy, 2015; Dugord et al., 2014). Significant spatial variabilities of heat-related health impact were found in all the above cases which indicates that heat-related health risks are considerably varying from place to place because of the spatial heterogeneity of the urban physical environment. The spatial uncertainty introduced by taking the entire city as a whole in health burden assessment will lead to large bias.

Hong Kong is a large city situated at the southeast side of the Pearl River Delta (PRD) region of China (Fig. 2). It has a total area of about 1104 km<sup>2</sup>, owing to its mountainous topography with steep slopes over 20% of the total land area, most of the urban activities are concentrated on built-up areas which take up about 24% of land (DEVB, 2017). The population of more than seven million makes Hong Kong one of the densest cities worldwide. Hong Kong has a typical sub-tropical maritime climate based on the Köppen-Geiger Climate Classification (Peel et al., 2007). It features hot and humid summer season (June to August) with a seasonal averaged air temperature of 23.4 °C and a mean relative humidity of approximately 81%. The average annual precipitation in Hong Kong is about 2400 mm (HKO, 2015).

Under the combined effect of global climate change and local urbanization, there is a long term increasing trend in the average temperature in Hong Kong. Moreover, Hong Kong is experiencing an increasing influence of extreme hot weather (Wang et al., 2016; Chan et al., 2012; Wong et al., 2011). The prolonged period of extreme hot weather has led to severe health issues in recent years (Ho et al., 2017; Sham, 2015). Since an earlier study on investigating the weather-mortality relationship (Yan, 2000) was conducted, there have been several studies focusing on the correlation between the health burdens and hot weather conditions (Goggins et al., 2012a, 2012b; Chan et al., 2012). An evaluation indicator, Hong Kong Heat Index (HKHI), has been developed by the Hong Kong Observatory (HKO) to cater for the humid and hot summer condition in Hong Kong and adopted to enhance the heat stress information services in Hong Kong (Lee et al., 2016). However, a limitation still exists, which is that the time-series analysis does not fully consider spatial factors due to complex topography and urban environment. It has been observed that the complex urban land use and surface characteristics of Hong Kong lead to a significant intra-urban spatial variability in climate (Shi et al., 2017). Using a UHI intensity index (UHII), Goggins et al. (2012a, 2012b) proved that the temperature-related mortality in those areas with a high UHI intensity is higher than the areas with a low UHI intensity. However, simply referencing the air temperature measured by the nearest weather station (WS) still introduce large uncertainties and

biases into the heat-related health impact assessment. The above indicates that a comprehensive spatial understanding of the extreme hot weather events is urgently needed for urban heat disaster prevention and public health management of Hong Kong. The urban topography is also a major modifying factor of the spatial characteristic of urban climate (Ketterer and Matzarakis, 2014). The complex land surface morphology changes the atmospheric conditions at different spatial scales (Raupach and Finnigan, 1997), which will consequently alter the spatial pattern of air temperature (Draxler, 1986). The interaction between the mountainous topography and the urban boundary layer climate is complicated and vary at different places in Hong Kong (Tong et al., 2005). Therefore, it is helpful to take the land surface morphology into account, while investigating the spatial variability of the extreme hot weather.

As a robust and widely used technique for the spatial mapping of environmental exposure, land use regression (LUR) model has been applied for investigating the spatial variability of the environmental exposure of the air pollution (Ryan and LeMasters, 2007), heat (Shi et al., 2018) and noise (Xie et al., 2011). Using onsite measured data, an LUR model assesses the environmental exposure level (outcome variables) at unmeasured places by considering the land use composition, population density and other urban configurations as the predictors. The dependence on data makes the LUR a data-intensive method. Taking the advantage of the extensive input dataset, LUR modelling enables a fine-scale spatial estimation for unmeasured areas when dealing with the geographic heterogeneity in large cities. It has been found that LUR usually has a slightly better performance when compared with other geostatistical methods for spatial assessment (Hoek et al., 2008; Adam-Poupart et al., 2014).

In this paper, we investigate the spatial pattern of the summertime extreme hot weather condition via LUR modelling in the complex heterogeneous geographic context of Hong Kong. Besides all conventionally used LUR predictors (Ryan and LeMasters, 2007), land surface morphology was also quantified and adopted as the predictor variables by this study to enhance the robustness of LUR models of the extreme hot weather. Adopting the LUR modelling technique, we aim to map the spatial pattern of the summertime extreme hot weather of Hong Kong at the community level, using two indicators – annual VHDHs and annual HNHs.

## 2. Materials and methods

In this study, the spatial variation in the summertime extreme hot weather events (both daytime and nighttime) was investigated based on a 5-year (2011–2015) hourly air temperature records from a total of 40 WSs maintained by the Hong Kong Observatory (HKO), the meteorological authority in Hong Kong. A set of conventionally used LUR predictor variables (include but not limited to land use, population density, elevation) were extracted and generated using the land use and urban configuration information. The heterogeneous land surface morphology was quantified by a set of urban morphological/morphometrical indexes. These indexes were further collated in the geographical information system (GIS) and processed into a series of geographic information layers. Data extracted from these layers at a set of LUR buffer widths of the WSs' locations were also incorporated into the LUR models as predictor variables. Fig. 1 provides a flow diagram of the method used in this study.

### 2.1. LUR outcome variables – quantifying the extreme hot weather condition

The case city investigated in this study is Hong Kong. The weather of Hong Kong has a considerable spatial variability due to the effects of the mountainous topography, complex land surface and urban morphology as well as the circulation of land - sea breeze (Chin, 1986; Yan, 2007; Mok et al., 2011). Under the circumstance of climate change and

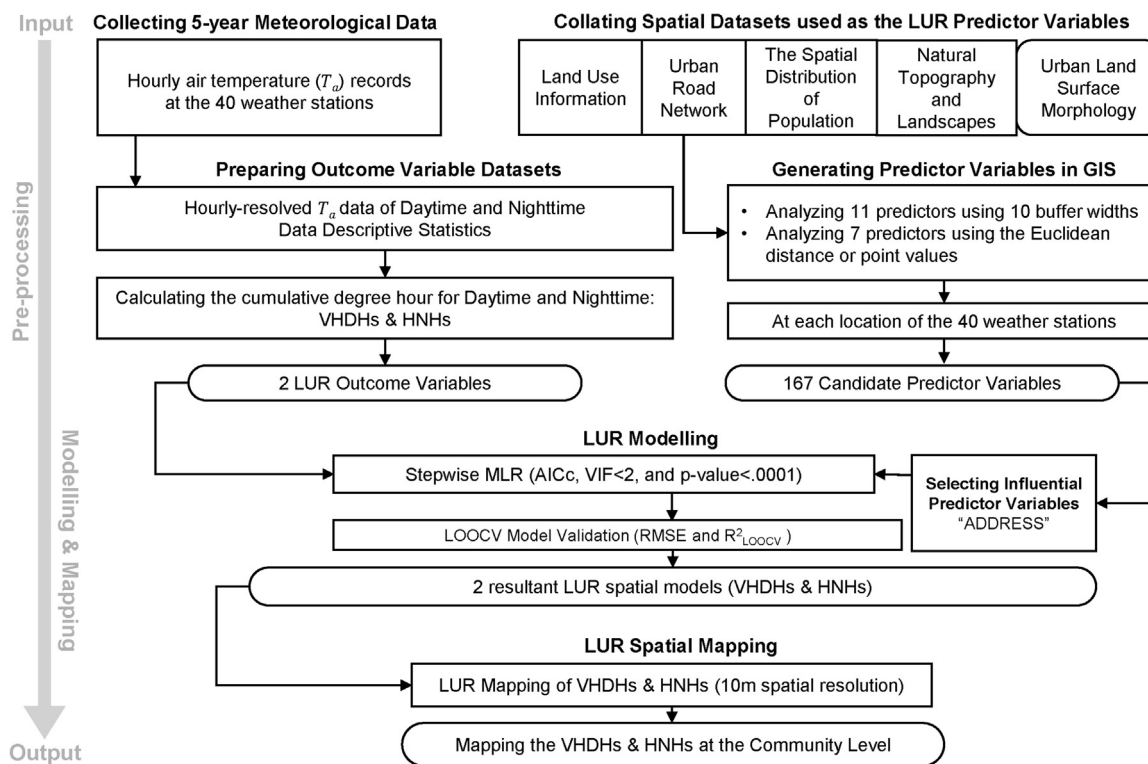


Fig. 1. The flow diagram of the method used in this present study.

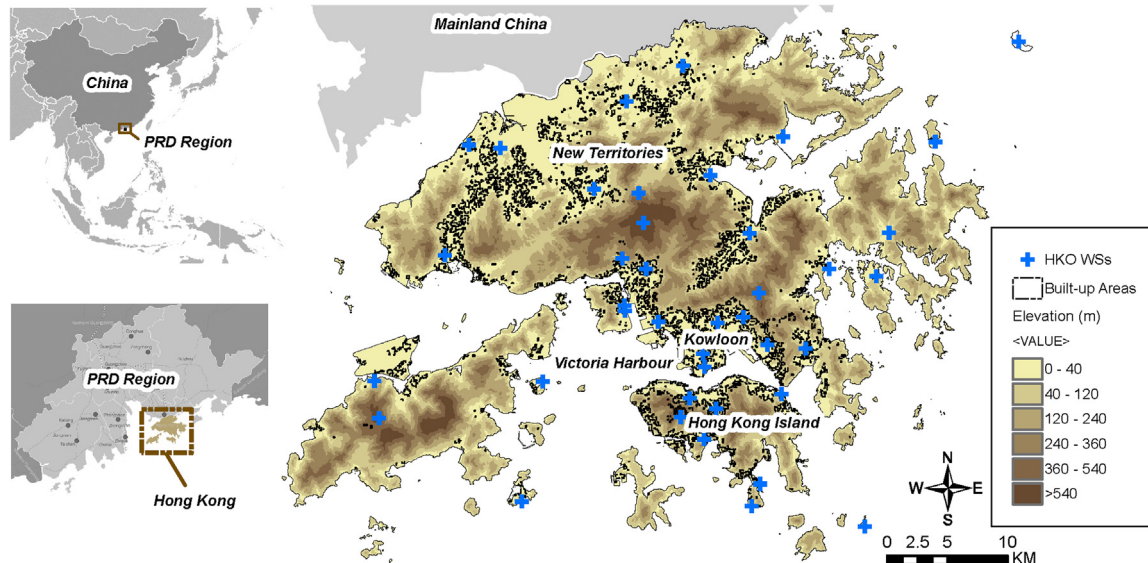
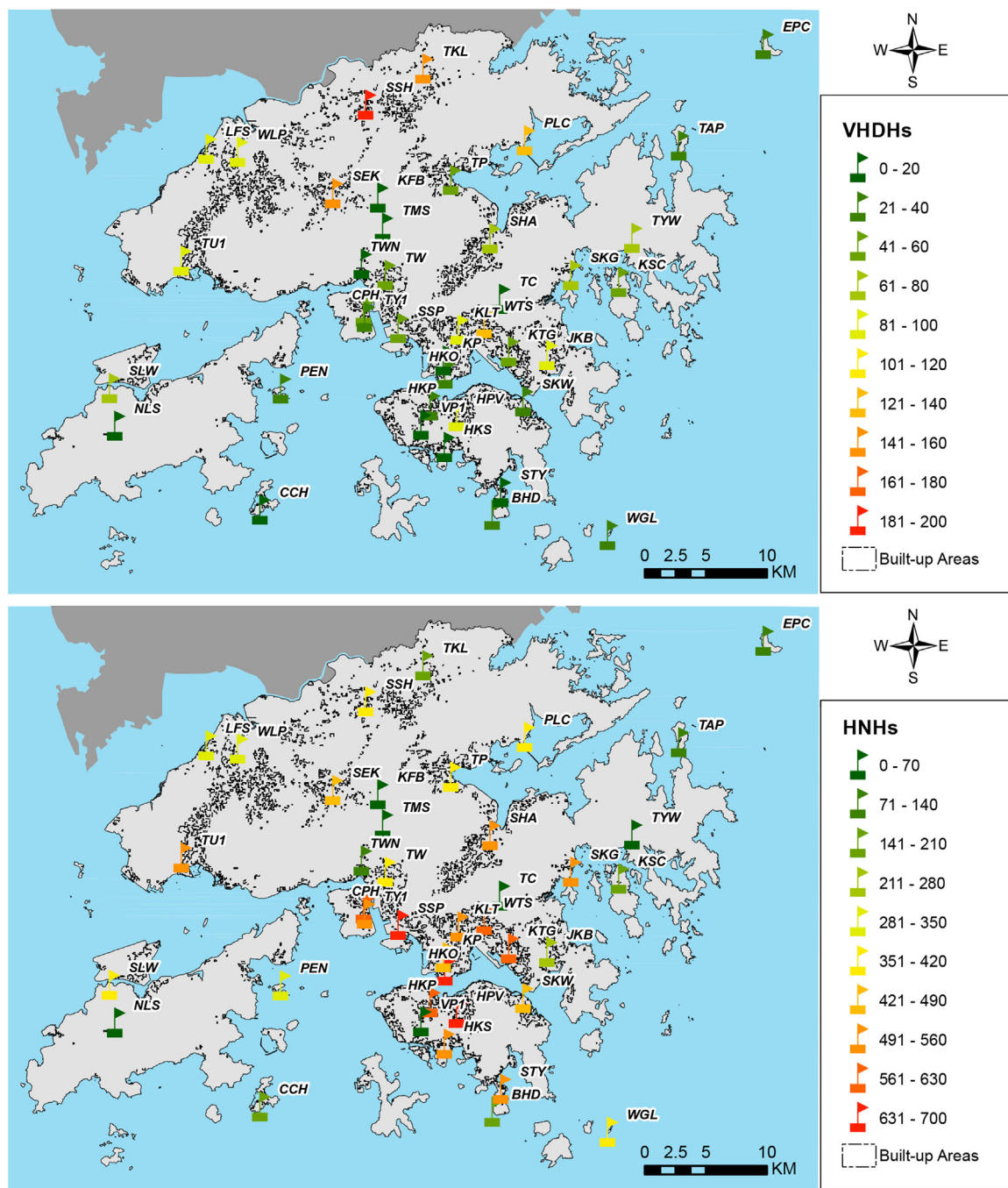


Fig. 2. The study area and the 40 WSSs of the HKO weather monitoring network in Hong Kong.

local urbanization, the rate of increase in annual average air temperature became faster in the recent decades in Hong Kong (Leung et al., 2004; Wing-lui et al., 2010). To investigate and represent the most recent weather condition of Hong Kong, a 5-year (2011–2015) hourly air temperature ( $T_a$ , °C) dataset monitored by a total of 40 WSSs (Fig. 2) was acquired from the HKO as the basis of quantifying the extremely hot weather conditions. The relevant metadata of the  $T_a$  datasets were also collected, which are including but not limited to the geographic locations, elevations and the neighbouring environment of each WS (HKO, 2017b).

In this study, based on the HKO weather records, two extreme hot weather condition indicators – VHDHs and HNHs were used as the outcome variables of the LUR modelling. The extreme hot weather

events are commonly quantified by the intensity and duration (Anderson and Bell, 2011). The two indicators used in this study are developed based on the concept of the cumulative degree hour (simply speaking, the amount of hot hours, hereafter referred HHs) adopted in a previous research (Macnee and Tokai, 2016) and the general definition of very hot days and hot nights adopted by HKO (2017a). The VHDHs refers to the total number of hours greater than or equal to 33 °C during the day (7:00–18:00 HKT). The HNHs refers to the total number of hours greater than or equal to 28 °C at night (1:00 – 6:00 and 19:00 – 24:00 HKT). VHDHs and HNHs were calculated for the entire summer of Hong Kong which define as the period from June to August (Sham, 2015). (Fig. 3).



**Fig. 3.** The spatial pattern of the 5-year averaged annual VHDHs (upper) and HNHs (below) at the locations of WSs in Hong Kong. The flags in the figure represent the WS locations. The colour scale represents the numbers of VHDHs and HNHs (unit: hour). (For interpretation of the references to color in this figure legend, the reader is referred to the web version of this article.)

## 2.2. LUR predictor variables

Five categories of data/information were collected and collated in the GIS as the predictor variables for the development of the LUR model of the VHDHs and HNHs: (1) land use information, (2) urban road networks, (3) the spatial distribution of population, (4) natural topography and landscapes, and (5) urban land surface morphology. A total of ten different buffer widths, range from 100 m (which is a spatial scale of a small street block) to 3000 m (represent the spatial scale of a district) were used for generating predictor variable datasets. The data processing of the first four categories of the predictor variables datasets is explained in details in the [Supplementary material](#) of this article, as

they have been widely used in LUR modelling studies. Different from most of the previous LUR studies, in the present study, the urban land surface morphology is also quantified and included as the predictor variables.

The spatial pattern of UHI is significantly affected by the near-surface wind field, which is highly related to the land surface morphology. The near-surface wind field is largely determined by the interactions between the land surface and the atmosphere (Arnfield, 2003). In the complex urban context of Hong Kong, the land surface morphology varies at different places. Such spatial heterogeneity in land surface morphology leads to a complex spatial variability in the air pressure (Landsberg, 1981). For example, the hilly topography has a substantial

influence in the air flow (Lai et al., 2014). Moreover, it has long been emphasized that the building density and building arrangement significantly affect the urban ventilation (Bottema, 1997; Franck et al., 2013; Clarke, 1972). Therefore, it could be beneficial to analyse and incorporate the land surface morphology as the predictors for investigating the spatial pattern of the extreme hot weather condition. By means of GIS, the geomorphometrical analysis has been widely adopted in the topoclimatological research (Böhner and Antonić, 2009). In this present study, a set of land surface morphological indexes were adopted as the predictor variables. Three building parameters - building volume density ( $\sigma_{Bldg}$ ), sky view factor ( $\Psi_{SVF}$ ), frontal area ratio ( $\lambda_F$ ) were used to depict the land surface morphology of built environment in the high-density intraurban area. Rainfall is also an important meteorological factor in mitigating heat waves (Wilby, 2007; Lam et al., 2012). Windward-leeward index ( $WLI$ ), as a commonly-used geomorphometrical predictor of wind and precipitation (Bohner, 2006), was selected to consider the topographical effect of the mountainous geomorphology. Above variables have been confirmed to be effective to represent the complex near-surface wind condition of Hong Kong (Shi et al., 2017).

$\sigma_{Bldg}$  is a dimensionless ratio ranges from 0 to 1, which measures of the relative building density of a site based on the overall urban density level of an entire study area. Assume that there is a total of  $m$  sites in the study area and there is a total of  $n$  buildings in each of these  $m$  sites, the total building volume in site  $j$  ( $V_j$ ) was calculated using Eq. (1), where  $A_{Pi}$  is the footprint area of the building  $i$ .  $h_i$  is the building height of the building  $i$ . The  $\sigma_{Bldg,j}$  is defined as the ratio of  $V_j$  to the calculated maximum building volume ( $V_{max}$ ) in the entire study area (Eq. (2)):

$$V_j = \sum_{i=1}^n A_{Pi} h_i \quad (1)$$

$$\sigma_{Bldg,j} = \frac{V_j}{V_{max}} \quad (2)$$

$\Psi_{SVF}$ , as a dimensionless ratio ranges from 0 to 1, describes the openness of a near-surface point location to the sky hemisphere (Watson and Johnson, 1987). It was commonly recognized and used as a proxy of the incoming shortwave solar radiation and intraurban air temperature differences (Svensson, 2004). In this study, a high-resolution (2 m-resolution) digital terrain model (DTM) (Fig. 4) of Hong Kong was created by combining the digital elevation data and the building surveying data. The  $\Psi$  was calculated at each single point of the DTM surface by following the calculation method by Dozier and Frew (1990). The detailed geometry calculation has been mentioned in their article:

$$\Psi_{SVF} = \frac{1}{2\pi} \int_0^{2\pi} [\cos\beta \cos^2\varphi + \sin\beta \cdot \cos(\Phi - \alpha) \cdot (90 - \varphi - \sin\varphi \cos\varphi)] d\Phi \quad (3)$$

$\lambda_F$  is defined as the ratio of the total projected frontal area of all buildings in a particular site to the total land area of the site. There are two commonly-used methods of site zoning for the calculation of  $\lambda_F$ , which are the orthogonal grid method (OGM) (Ng et al., 2011) and Thiessen polygon method (TPM) (Gál and Unger, 2009). In this study, the TPM was used due to the irregular building arrangements. Assume that there are a total of  $m$  sites in the entire study area,  $\lambda_{Fj}$  is the frontal area ratio of the site  $j$  in the study area.  $\lambda_{Fj}$  can be calculated by using Eq. (4), where  $n$  is the total number of buildings in the site  $j$ . The  $A_{Fi}$  is the projected frontal area of the building  $i$  under a prescribed wind direction ( $\theta$ ). Therefore, the total projected frontal area was calculated as  $\sum_{i=1}^n A_{Fi}$  (the overlapped projection of the building frontal area between buildings was only calculated for once). Using the one-hour mean wind direction records from the nearest weather station operated by HKO, the 16-wind direction probability-weighted frontal area ratio  $\bar{\lambda}_F$  can be then calculated via Eq. (5).

$$\lambda_{Fj} = \left( \sum_{i=1}^n A_{Fi} \right) / A_{Tj} \quad (4)$$

$$\bar{\lambda}_F = \sum_{\theta=1}^{16} \lambda_{Fj(\theta)} \cdot P_{(\theta)} \quad (5)$$

$WLI$  (ranges from 1, represent a fully windward position to the value of -1, which is a leeward position) is a land surface morphological parameter that describes the spatial relationship between the land surface angular slope and a prescribed wind direction (Böhner and Antonić, 2009). The  $WLI$  value at a particular location in the DTM surface data under the condition of a prescribed wind direction ( $\theta$ ) was calculated via Eq. (6), Eq. (7), and Eq. (8) based on the windward and leeward horizon parameter function, which are  $H_\varphi$  and  $H_\eta$  respectively (Bohner, 2006; Huang, 2017). For a particular location in the DTM surface,  $\Delta h_{\varphi i}$  and  $\Delta h_{\eta i}$  are the horizontal distances in the windward and leeward direction, while  $\Delta z_{\varphi i}$  and  $\Delta z_{\eta i}$  are the vertical distances in the windward and leeward direction respectively. More details can be found in Huang (2017). The calculation was completed in the open source package SAGA GIS (Olaya, 2004) in this study. Similar with the calculation of the  $\bar{\lambda}_F$ , the 16-wind direction probability-weighted  $WLI$  ( $\bar{WLI}$ ) was calculated for the entire area of the DTM of Hong Kong (Eq. (9)).

$$H_\varphi = \frac{\sum_{i=1}^n \frac{1}{\Delta h_{\varphi i}} \cdot \tan^{-1} \left( \frac{\Delta z_{\varphi i}}{\Delta h_{\varphi i}^{0.5}} \right)}{\sum_{i=1}^n \frac{1}{\Delta h_{\eta i}}} + \frac{\sum_{i=1}^n \frac{1}{\Delta h_{\eta i}} \cdot \tan^{-1} \left( \frac{\Delta z_{\eta i}}{\Delta h_{\eta i}^{0.5}} \right)}{\sum_{i=1}^n \frac{1}{\Delta h_{\eta i}}} \quad (6)$$

$$H_\eta = \frac{\sum_{i=1}^n \frac{1}{\ln(\Delta h_{\eta i})} \cdot \tan^{-1} \left( \frac{\Delta z_{\eta i}}{\Delta h_{\eta i}^{0.5}} \right)}{\sum_{i=1}^n \frac{1}{\ln(\Delta h_{\eta i})}} \quad (7)$$

$$WLI_{(\theta)} = H_\varphi \cdot H_\eta \quad (8)$$

$$\bar{WLI} = \sum_{\theta=1}^{16} WLI_{(\theta)} \cdot P_{(\theta)} \quad (9)$$

### 2.3. LUR modelling

#### 2.3.1. LUR buffering analysis

Except for the distance-based and point-based predictors, all the other predictor variables were calculated using buffering analysis. Buffering analysis is a widely-used geospatial analysis method in GIS, which defines a zone around a location of interest using a specific width. In this study, ten different LUR buffering widths (100 m, 200 m, 300 m, 400 m, 500 m, 750 m, 1000 m, 1500 m, 2000 m, and 3000 m). As the results, a total of 167 candidate predictor variables were considered in this study. Table 1 shows a full list of all candidate predictor variables involved in the LUR modelling process of this study.

#### 2.3.2. Influential predictor variables - “ADDRESS” selection

The commonly adopted stepwise regression (Tabachnick and Fidell, 2001) was used for the LUR model development of this present study. LUR modelling is essentially a multiple linear regression (MLR) process. It has known that involving too many input predictors during the multiple linear regression modelling leads to collinearity, which further causes over-fitting problems and spurious resultant regression models (Tu et al., 2005). Therefore, for this present study, it is beneficial to perform a pre-screening of the complete predictor variable set to reduce the number of the final input variables for the next-step LUR modelling. Therefore, a practical and efficient variable screening method – the “A Distance Decay REgression Selection Strategy (ADDRESS)” developed by Su et al. (2009b) was adopted in this study. This method is essentially a sensitivity test for each buffer-based predictor variable to test the sensitivity of the variables to different buffers and identify the critical buffer(s) for each variable. To perform the sensitivity test for a particular predictor variable ( $VAR_i$ ), first, a group of simple linear regression models was developed using the ten buffer widths. The models could be represented by two common equations:

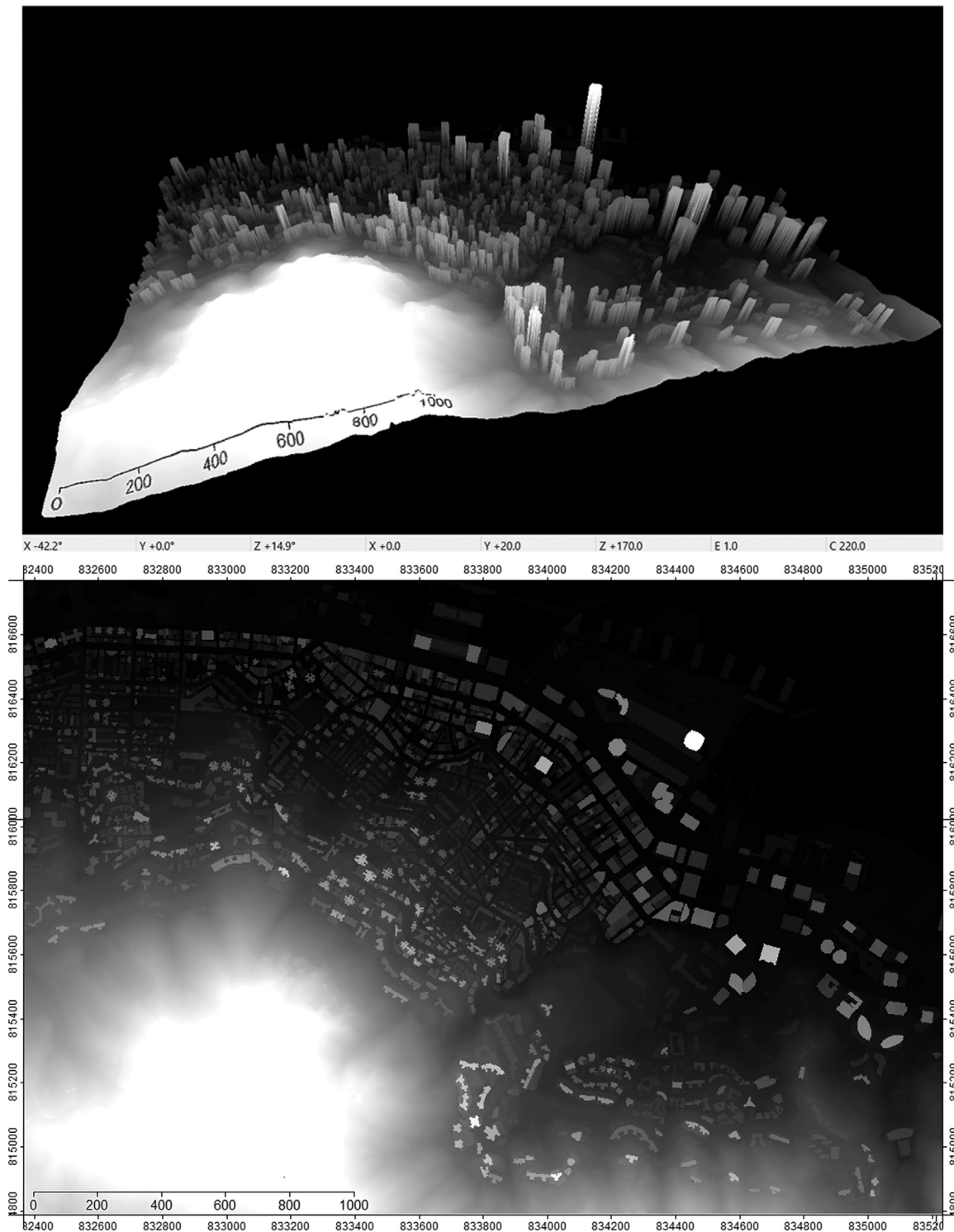


**Fig. 4.** A 3D view (upper) and plan view (below) of a sample of the input high-resolution DTM data of Hong Kong.

$$VHDHs_i = \alpha_{ij} VAR_{test,buffer_j} + \beta_{ij} \quad (10)$$

$$HNHs_i = \alpha_{ij} VAR_{test,buffer_j} + \beta_{ij} \quad (11)$$

where  $VHDHs_i$  is the VHDHs at the location  $i$ .  $VAR_{test,buffer_j}$  is the testing variable calculated within the buffer width  $j$  (refers to the [Section 2.3.1](#) and [Table 1](#) for the value of  $j$ ).  $\alpha_{ij}$  is the model slope of the  $VAR_{test,buffer_j}$ .  $\beta_{ij}$  is the intercept of the model. The simple linear regression model was developed for each of the ten values of  $j$ . For each testing variable, ten simple linear regression models were developed (the resultant ten

models share the same model structure as indicated by Eq. (10)). A distance-decay curve (a function of buffer widths) was then plotted based on the ten corresponding Pearson correlation coefficients ( $R$ ) for each  $VAR_{i,buffer_j}$  ([Fig. 5](#)). The critical buffer widths (mainly the peaks and inflection points) of each buffer-based variable were identified by adopting As the results, only variables at the critical buffers were kept as the final input variables for next-step LUR modelling. The same pre-screening procedure was repeated for another outcome variable – HNHs (Eq. (11)).

**Table 1**

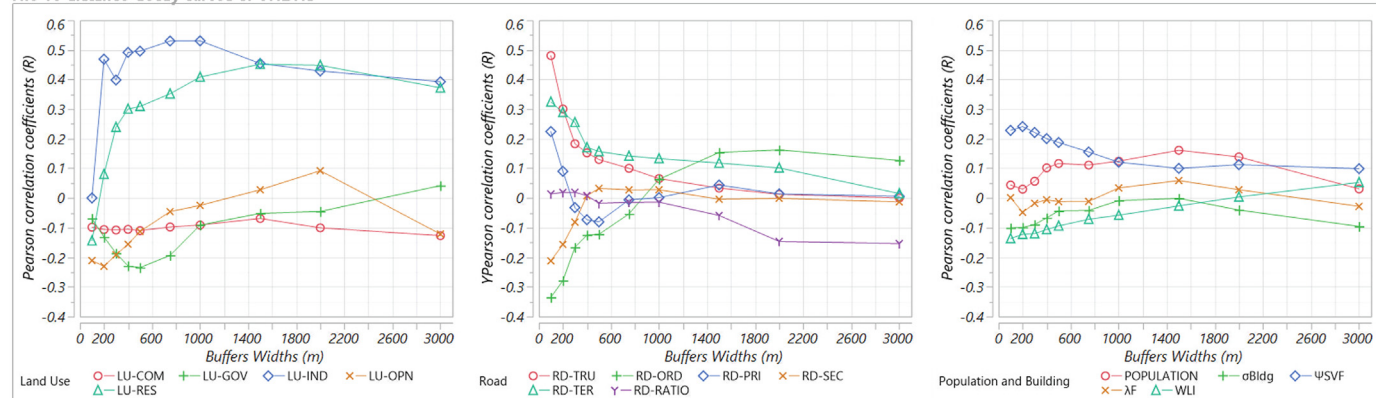
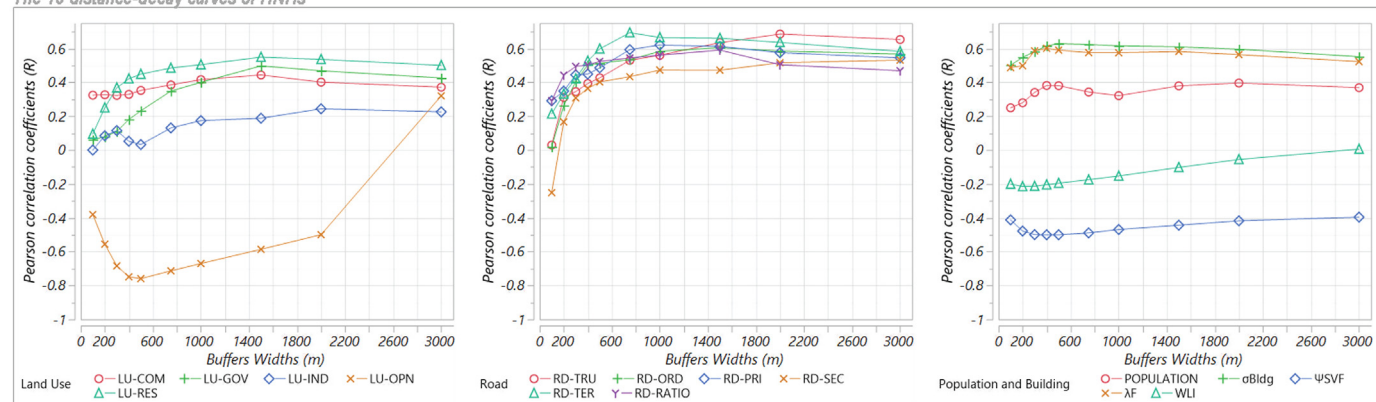
A full list of all candidate predictor variables involved in the LUR statistical modelling process of this study.

Predictor Variables	Variables' Units	Geospatial Analysis Methods	Variables' Code
<b>Land Use Information</b> (refer to Section 1 of the Supplementary material)			
Total area within the buffer	m <sup>2</sup>	Buffer <sup>a</sup>	LU-RES
Residential land use	m <sup>2</sup>	Buffer	LU-COM
Commercial land use	m <sup>2</sup>	Buffer	LU-IND
Industrial land use	m <sup>2</sup>	Buffer	LU-GOV
Government land use	m <sup>2</sup>	Buffer	LU-OPN
Open space land use	m <sup>2</sup>	Buffer	
<b>Urban Road Network</b> (refer to Section 2 of the Supplementary material)			
Road network line density	Trunk road/expressways km/km <sup>2</sup>	Buffer	RD-TRU
Primary road	km/km <sup>2</sup>	Buffer	RD-PRI
Secondary road	km/km <sup>2</sup>	Buffer	RD-SEC
Tertiary road	km/km <sup>2</sup>	Buffer	RD-TER
Ordinary road	km/km <sup>2</sup>	Buffer	RD-ORD
Road area ratio (%)	Standardized to [0–1]	Buffer	RD-RATIO
<b>The Spatial Distribution of Population</b> (refer to Section 3 of the Supplementary material)			
Population density	people per km <sup>2</sup>	Buffer	POPULATION
<b>Natural Topography and Landscapes</b> (refer to Section 4 of the Supplementary material)			
Geo-location (HK1980)	Longitude Latitude Elevation	Point	X Y Z
Distance to the nearest sources	Waterbody and waterfront Artificial urban parks Natural forestry areas	Distance	D-WATER D-PARK D-FOREST
<b>Urban Land Surface Morphology</b> (refer to Section 2.2) <sup>b</sup>			
Building volume density	Standardized to [0–1]	Buffer	$\sigma_{Bldg}$
Sky view factor	Standardized to [0–1]	Buffer, Point <sup>c</sup>	$\Psi_{SVF}$
Frontal area ratio	Dimensionless	Buffer	$\lambda_F$
Windward-leeward index	Dimensionless	Buffer	WLI

<sup>a</sup> A total of ten buffer widths were used: 100 m, 200 m, 300 m, 400 m, 500 m, 750 m, 1000 m, 1500 m, 2000 m, 3000 m.

<sup>b</sup> Variables depended on a prescribed wind direction were calculated based on the HKO meteorological records.

<sup>c</sup> Originally,  $\Psi_{SVF}$  is developed for a point location. Therefore, besides the averaged  $\Psi_{SVF}$  in different buffer widths, point  $\Psi_{SVF}$  values at each the location of each WS were defined as the variable within a 0 m buffer and used as a predictor variable in this study as well.

**The 16 distance-decay curves of VHDHs****The 16 distance-decay curves of HNHs**

**Fig. 5.** The 32 distance-decay curves of Pearson correlation coefficients between all buffer-based variables and VHDHs/HNHs.

### 2.3.3. Stepwise regression LUR modelling and model cross validation

Stepwise regression technique has been widely applied for screening predictor variables for the multivariate analyses (Jenrich, 1977; Miller, 1984; Miller, 2002). In this present study, SAS JMP statistical software was used to select predictor variables and optimize the LUR models (Freund et al., 2003; Sall et al., 2012). The minimum Akaike information criterion (AIC) is one of the most widely-used criteria in stepwise MLR. In this study, it was used to determine the optimal LUR models of the VHDHs and HNHs. The variance inflation factor (VIF) was calculated for each predictor variables of the developed models. The criteria of  $VIF < 2$  was applied to exclude those predictor variables with significant collinearity before constructing the final LUR models. For each of the developed LUR models, the adjusted  $R^2$  ( $\bar{R}^2$ ) values were checked to evaluate the prediction performance. Leave-one-out cross validation (LOOCV) was also performed to examine the resultant models (both the  $RMSE_{LOOCV}$  and the  $R^2_{LOOCV}$  were calculated for each resultant model). The structure of the resultant LUR models of the VHDHs (Eq. (12)) and HNHs (Eq. (13)) can be illustrated as the following equation:

$$VHDHs_i = \alpha_1 VAR_{1j1} + \alpha_2 VAR_{2j2} + \dots \alpha_n VAR_{njm} + \beta_i + \varepsilon \quad (12)$$

$$HNHs_i = \alpha_1 VAR_{1j1} + \alpha_2 VAR_{2j2} + \dots \alpha_n VAR_{njm} + \beta_i + \varepsilon \quad (13)$$

where  $VHDHs_i$  and  $HNHs_i$  are the VHDHs and HNHs at the location  $i$ .  $VAR_{1j1}, VAR_{2j2}, \dots, VAR_{njm}$  are the predictor variables calculated within the buffer width  $j1, j2, \dots, jm$ .  $\alpha_1, \alpha_2, \dots, \alpha_n$  are the corresponding correlation coefficients of the predictors.  $\beta_i$  is the model intercept.  $\varepsilon$  is the model residual.

## 3. Results and discussions

### 3.1. Influential predictor variables at the critical buffers

As described in the methodology section, the “ADDRESS” method (Su et al., 2009a) was adopted by this present study as the method of the sensitivity test of buffer widths and the influential predictor variable selection. As the results, a total of 32 distance-decay curves were created to understand the correlation between the predictors and outcome variables (Fig. 5). Based on these distance-decay curves, the critical buffer widths of each variable were identified (Table 2). There are some common influential variables between VHDHs and HNHs. These

variables share the similar effects on the HHs between daytime and nighttime. These variables include the land use-related variables LU-RES, LU-IND, LU-OPN, the POPULATION, and the road network-related variables RD-TRU, RD-PRI, RD-TER. Both LU-RES and LU-IND have a positive correlation with the HHs, while the correlation between LU-OPN and HHs is negative. LU-RES and LU-IND portray the spatial distribution of the building-related anthropogenic heat sources. High emission intensity of the anthropogenic heat aggravates the HHs in both daytime and nighttime. Similarly, the RD-TRU, RD-PRI, RD-TER are also positively correlated with the HHs because of the vehicular heat exhaust. The POPULATION has the same critical buffer width of 1500 m with LU-RES, which is as expected because the population census data should be consistent with the layout of residential land use area in the city. WLI, as a land surface morphological parameter, reflects the wind availability. A larger WLI value at a location indicates a better ventilation (more air flows), which further implies a lower possibility of the heat aggregation at that particular location. Therefore, the WLI has a negative correlation with both the VHDHs and HNHs as expected.

Daytime-nighttime differences have been observed in some other influential variables. For example, the land surface morphological parameters  $\sigma_{Bldg}$  and  $\Psi_{SVF}$ , and also land use variables LU-COM and LU-GOV. These variables have the opposite correlation with the VHDHs and HNHs.  $\sigma_{Bldg}$  has a negative correlation with the VHDHs because during the daytime, building clusters with a larger density blocks most of the incoming solar radiation from the open sky, consequently reduce the accumulation of the heat within the street (Yang et al., 2017). However, a larger building volume also absorbs more shortwave solar radiation during the daytime and thus stores more heat. During the nighttime, the heat is released from the buildings in the form of long-wave radiation. It is trapped by the dense building clusters and increases the temperature of the ambient air volume (Nunez and Oke, 1977). The effect of  $\Psi_{SVF}$  is similar to the  $\sigma_{Bldg}$  but works in an opposite way because a larger  $\Psi_{SVF}$  allows more incoming solar radiation during the daytime and could be helpful to the nighttime heat dissipation (Oke, 1981). LU-COM negatively correlates with VHDHs and positively correlates with HNHs, which is possibly because that the built environment of the commercial land use areas in Hong Kong usually have a very large building volume (due to the extremely high land price and the commercial value). The effect of LU-COM is more similar with the  $\sigma_{Bldg}$  due to the influence of the building volume. LU-GOV also has different

**Table 2**

The sensitivity test results of the critical buffer widths for each buffer-based variable and the selection of influential predictor variables for the stepwise regression modelling input.

Outcome Variables	VHDHs				HNHs			
	Predictor Variables	Critical Buffer (m)	Correlation	Used as the Modelling Input	Critical Buffer (m)	Correlation	Used as the Modelling Input	
LU-RES	1500	positive	Y		1500	positive	Y	
LU-COM	500	negative	Y		1500	positive	Y	
LU-IND	1000	positive	Y		2000	positive	Y	
LU-GOV	500	negative	Y		1500	positive	Y	
LU-OPN	200	negative	Y		500	negative	Y	
RD-TRU	100	positive	Y		2000	positive	Y	
RD-PRI	100	positive	Y		1000	positive	Y	
RD-SEC	n.a	n.a	N		n.a	n.a	N	
RD-TER	100	positive	Y		750	positive	Y	
RD-ORD	n.a	n.a	N		400	positive	Y	
RD-RATIO	n.a	n.a	N		1500	positive	Y	
POPULATION	1500	positive	Y		1500	positive	Y	
$\sigma_{Bldg}$	100	negative	Y		500	positive	Y	
$\Psi_{SVF}$	200	positive	Y		400	negative	Y	
$\lambda_F$	n.a	n.a	N		400	positive	Y	
WLI	100	negative	Y		200	negative	Y	

Notes:

“n.a”: The correlation changes between positive and negative with the increase of buffer widths. The variable will not be used as the modelling input.

“Y”: The variable was used as the modelling input.

“N”: The variable was not used as the modelling input.

correlations with VHDHs and HNHs during the daytime and nighttime.

Besides the LU-RES and POPULATION, all other variables have different critical buffer widths between the VHDHs and HNHs. The differences in the critical buffers of the urban land surface morphological variables ( $\sigma_{Bldg}$ ,  $\Psi_{SVF}$ , and  $WLI$ ) could be explained by the differences in the atmosphere-land surface energy balance during the daytime and nighttime (Oke, 1988). Although there are slight differences, the critical buffers of  $\sigma_{Bldg}$ ,  $\Psi_{SVF}$ , and  $WLI$  all have a relatively small spatial scale of 100–400 m, which is basically at the urban neighborhood scale. Such findings indicate that the effect of radiation and air flow on the VHDHs and HNHs could only be effectively evaluated by fine-scale investigations. For all other land use and road network-related variables, the critical buffers of the HNHs are larger than the VHDHs, which indicates that the urban setting/configurations have a larger sphere of influence on the HNs during the nighttime than the daytime, which indicates a stronger influence. Some of the variables have a correlation changes between positive and negative with the increase of buffer widths. These variables were not used as the input data of the stepwise regression modelling.

### 3.2. Resultant LUR models of VHDHs and HNHs

Using the influential predictor variables that identified in Section 3.1 (Table 2), the LUR models of the VHDHs and HNHs were developed (Eq. 14 and Eq. 15 in Table 3 and Fig. 6). The two resultant LUR models meet the requirements that: (1) the model and all model predictor variables have a significant level of p-value smaller than 0.0001; (2) all model predictor variables meet the criteria of VIF less than 2.

### 3.3. Spatial mapping of VHDHs and HNHs

On top of the resultant LUR models, the spatial mapping was performed for the VHDHs and HNHs respectively. First, all predictor variables included in the two resultant LUR models were calculated for each location within the land area of Hong Kong in GIS. As the results, seven geographical raster layers were generated. The spatial mapping of VHDHs and HNHs were then performed based on the resultant LUR models shown in Table 3. Considering the study area has a total area of

**Table 3**

The resultant LUR models of VHDHs and HNHs (all models and predictors meet the criteria of  $p < .0001$  and  $VIF < 2$ ).

#### Resultant LUR Model of VHDHs

Outcome Variable	VHDHs
$R^2$	0.742
$\bar{R}^2$	0.712
$RMSE_{LOOCV}$	23.86
Mean of Outcomes	52.59
p-value	< .0001
$R^2_{LOOCV}$	0.706
Model Structure	

$$VHDHs = (-1.470e-4)*LU\_GOV_{500m} + 8.898*RD\_EXP_{100m} - 0.154*Z + (1.534e-4)*LU\_OPN_{500m} + 75.716*RD\_TER_{750m} - 0.144*Z + 279.380*LU\_RES_{400m} + 0.199*D\_WATER \quad (14)$$

#### Resultant LUR Model of HNHs

Outcome Variable	HNHs
$R^2$	0.822
$\bar{R}^2$	0.801
$RMSE_{LOOCV}$	95.057
Mean of Outcomes	349.81
p-value	< .0001
$R^2_{LOOCV}$	0.767
Model Structure	

$$HNHs = (-5.110e-4)*LU\_OPN_{500m} + 75.716*RD\_TER_{750m} - 0.144*Z + 279.380*LU\_RES_{400m} + 0.199*D\_WATER \quad (15)$$

more than 1000 km<sup>2</sup>, a spatial resolution of 10 m was applied for all the mappings in this study to balance the mapping precision and the size of the database files. For the urban context of Hong Kong, a spatial resolution of 10 m would be fine enough for any further applications in the investigation of the extreme weather conditions and the assessment of heat-related health risks. The fine-scale resultant mapping could also be used as the background weather reference/input setting of the analysis of building energy consumption for the local sustainable building design practice. Fig. 7(a) and (c) shows the 10 m-resolution mapping results of the VHDHs and HNHs. To support public health preparedness, response and relief measures in the community level, the mapping results were further aggregated at the community level based on the zoning of SB/VC. Fig. 7(b) and (d) shows the final mapping results of the VHDHs and HNHs at the community level of Hong Kong.

## 4. Discussions

### 4.1. Findings and contributions

This present study measures and estimates the spatial pattern of the extreme hot weather condition of Hong Kong by using the VHDHs and HNHs based on weather observation in 2011–2015 as the indicators. Using LUR techniques, two statistical models of the VHDHs and HNHs were developed. For both of the two resultant models, only the four most influential and most contributing predictor variables were selected from an extensive set of candidate predictor variables. The  $\bar{R}^2$  of the VHDHs model and the HNHs model are 0.712 and 0.801 respectively. The two models also have a comparable  $R^2_{LOOCV}$  of 0.706 and 0.767 correspondingly, which confirms the robustness of the model prediction performance.

The VHDHs model contains the predictor variables of LU\_GOV<sub>500m</sub> (negative correlation with the VHDHs), RD\_EXP<sub>100m</sub> (positive correlation), Z (negative correlation), and D\_WATER (positive correlation). The presence of the LU\_GOV in the model is likely because government and community buildings in GIC sites are generally low- to mid-rise with better consideration of the surrounding environment. In Hong Kong, governmental projects take more environmental measures, which makes the government lands usually have a lower building density than other types of lands. Therefore, LU\_GOV to some extent reduce the possibility of heat accumulation and has a negative correlation with the VHDHs. This also indicates the effectiveness of the sustainable and environmental development strategies developed by the Hong Kong Building Department (BD) in recent years (BD, 2011a; b). These strategies are mandatory for most of the government development projects and aim to mitigate the impacts on urban climate due to urbanization and climate change. However, there are many different functions in governmental land areas – government, institution and community (GIC) sites of Hong Kong. Some are typical office buildings while the others are the 24-h operating public facilities. For those nighttime running facilities, the heat emission could be a possible explanation of the positive correlation between LU\_GOV and HNHs.

The positive correlation with RD\_EXP within a small buffer width implies the significant effect of vehicular heat exhaust within a short range (which can be clearly observed in Fig. 8). As indicated by a previous study in US (Hart and Sailor, 2009), road density is an important influencing factor of the local UHI intensity. It has been found that the air temperature above the major roads is closely related to the traffic-related anthropogenic activity. The consistency between the findings between the previous study and the present study indicate that the anthropogenic heat emission from the vehicular sector is still a determinant of UHI in Hong Kong despite the different urban scenario. The environmental benefits of the proximity to waterfront have been confirmed under the urban context of Hong Kong (Ng and Ren, 2015). The cooling effect of sea-breeze was revealed from the positive correlation between VHDHs and D\_WATER.

Different to the VHDHs, the HNHs were largely influenced by the

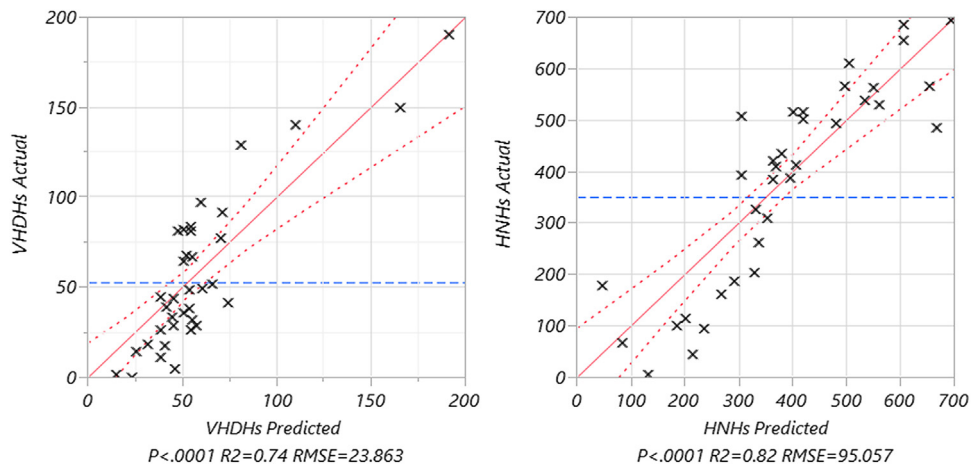


**Fig. 6.** The actual-by-predicted regression plot of the resultant LUR models of VHDHs (left) and HNHs (right). Each data point is corresponding to the validation of at the location of a weather station.

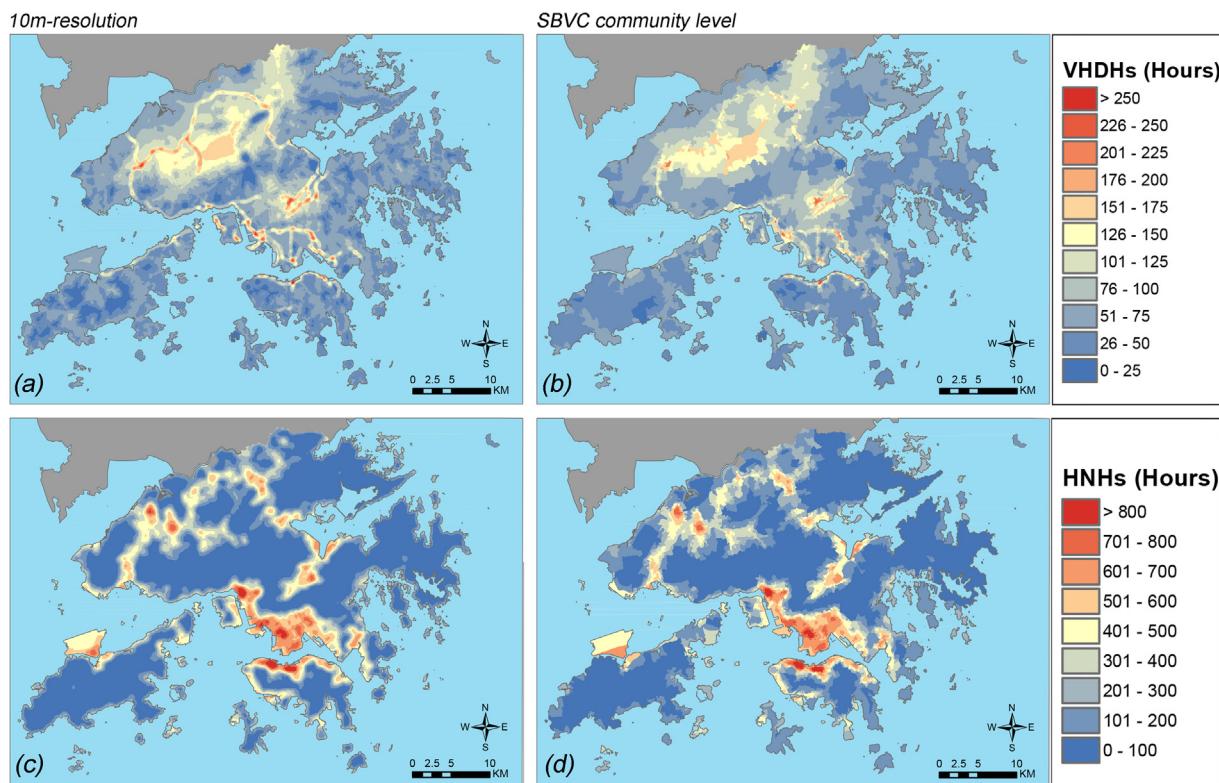


**Fig. 7.** The 10 m-resolution LUR mappings of the VHDHs (a) and HNHs (c) and the resultant spatial maps of the VHDHs (b) and HNHs (d) at the community level of Hong Kong.

heat dissipation rate during the nighttime. LU\_OPN<sub>500m</sub> and the building morphological parameter  $\lambda_{F400m}$  were proved to be the determining factors of the urban cooling and ventilation (Ng and Ren, 2015; Shi et al., 2017). Such influence can be clearly observed in Fig. 8. The resultant HNHs models prove that more open space and urban morphological permeability are helpful to the mitigation of the extreme hot weather conditions, especially in nighttime. The presence of the RD\_TER<sub>750m</sub> in the HNHs model is similar to the RD\_EXP<sub>100m</sub> in the VHDHs model. Both the VHDHs and HNHs have a negative correlation with the elevation Z, which is as expected because of the negative correlation between air temperature and altitude. It should be noticed that significant correlations between VHDHs/HNHs and WLI have been found, which confirms the importance of the wind in the heat dissipation. However, WLI finally being excluded from the resultant HNHs

model because of its collinearity with the other surface morphological variables.

The most important contribution of this present study is that it translates all qualitative common understandings into a set of comprehensive quantitative knowledge. The spatial pattern of the extreme hot weather events can be objectively and reasonably estimated not only for each community but also at a much finer spatial scale for Hong Kong at a higher level of robustness. As current ground-level weather station network do not extensively covered urban areas due to the limited land availability, there is a possible under-representation of urban effect in the temperature data and corresponding indicators of extreme hot weather (Szymanowski and Kryza, 2009). All above findings will contribute a more comprehensive spatial understanding of extreme hot weather conditions in a complex and heterogeneous

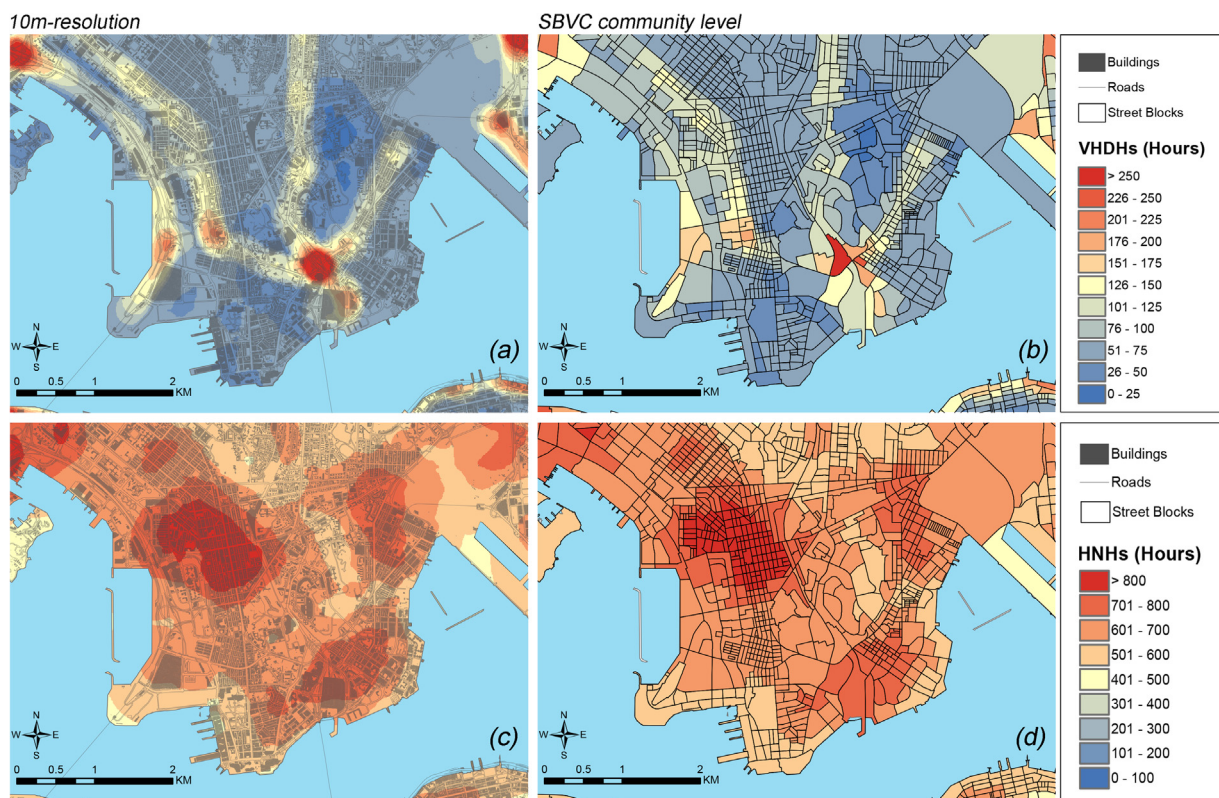


**Fig. 8.** The zoom-in 10 m-resolution LUR maps of the VHDHs (a) and HNHs (c) and the zoom-in resultant spatial maps of the VHDHs (b) and HNHs (d) at the community level of the high-density downtown area in Kowloon Peninsula.

geographic context of Hong Kong and form the scientific basis for future analysis when higher spatial resolution monitoring data is available. Such information will also be useful for identifying any sub-groups of the population that are at risk or vulnerable to such risks (Michelozzi et al., 2010) and improve the preparedness of extreme hot weather and associated response measures as well as the future enhancement of heat stress information services (WHO, 2008). The fine-scale spatial mapping can also be used as the background reference and help with better urban planning design and the analysis of building energy consumption for the local sustainable building design practices.

#### 4.2. Limitations and future works

Although the meteorological records used in this present study is a long-term hourly-resolved historical dataset of a period of 5 years, the total amount of WSs might be still limited and could not represent every type of the urban settings/configurations. The complicated hilly topography, heterogeneous land surface and building / street-level effects in Hong Kong make the local weather conditions vary significantly among different places. It is possible that there are still some other types of urban settings/configurations are not being investigated by the existing WSs yet. In future studies, the model performance could be potentially improved by setting up more short-term WSs to provide further information of the extreme hot weather condition in different places. Currently, this study already provides a fine-scale spatial understanding of the total amount of HHs during daytime and nighttime in summer for Hong Kong from a long-term perspective. The follow-up studies will focus on the mapping of the spatial pattern of the mean, minimum, maximum and hourly air temperature to further investigate the spatiotemporal variations of the extreme hot weather, which will allow a more detailed understanding/estimation of the extreme heat events, their potential impacts to various sectors of the society and to explore applications in location-specific weather forecasts that better take into consideration of the effects due to the urban settings/configurations.

#### 5. Conclusion

Investigating the spatial pattern of extreme hot weather condition at the community level is essential to the estimation of the heat-related vulnerability and relevant potential impacts to different sectors of the society. This study estimates the amount of summertime cumulative hot hours at the community level for daytime and nighttime respectively in Hong Kong. On the basis of the resultant LUR models (with the identifying the influential predictors), our findings have clearly showed that there are significant spatial variations in the extreme hot weather conditions in the territory and various land surface morphology indicators were identified as influential factors to the observed spatial variations.

The scholars, professionals and policy makers are increasingly becoming aware of the strong linkage between extreme hot weather and urbanization (Stone et al., 2010; ENB, 2017). Those quantitative relationships implied by the resultant models will provide useful references for stakeholders and policy makers to formulate relevant measures to adapt and mitigate various negative impacts of the extreme hot weather and improve the quality of living environment through integrating spatial climatic considerations in optimizing the urban planning and development, implementing environmental planning strategies and sustainable building design practices, and enhancing heat stress information services and related preparedness, response and relief measures in the community level. This is particularly essential for cities such as Hong Kong, where the large population and the compact building environment makes it more susceptible to extreme hot weather conditions (Ng et al., 2011). This study will help with the enhancement of Hong Kong's resistance to future extreme weather against the background of climate change and continuous city development.

#### Acknowledgement

This research is supported by the General Research Fund from Hong

Kong Research Grants Council (RGC-GRF No. 14611517, entitled “Climatic-responsive planning and action for mitigating heat-related health risk at community level in high density cities – A Case of Hong Kong”. This research is also supported by the Vice-Chancellor’s One-off Discretionary Fund of the Chinese University of Hong Kong and a collaboration project with Hong Kong Observatory, entitled “Investigating the Effect of Extreme Heat Events on Mortality and Potential Improvement to Existing Hot Weather Warning System in Hong Kong”. The authors especially wish to thank Mr. PW Chan of Hong Kong Observatory for his valuable advice on this study.

## Appendix A. Supporting information

Supplementary data associated with this article can be found in the online version at [doi:10.1016/j.enres.2019.01.041](https://doi.org/10.1016/j.enres.2019.01.041).

## References

- Adam-Poupart, Ariane, Brand, Allan, Fournier, Michel, Jerrett, Michael, Smargiassi, Audrey, 2014. Spatiotemporal modeling of ozone levels in Quebec (Canada): a comparison of Kriging, Land-Use Regression (LUR), and Combined Bayesian Maximum Entropy-LUR approaches. *Environ. Health Perspect.* 9 (122), 970–976. <https://doi.org/10.1289/ehp.1306566>.
- Anderson, G., Brooke, Bell, Michell L., 2011. heat waves in the United States: mortality risk during heat waves and effect modification by heat wave characteristics in 43 U.S. communities. *Environ. Health Perspect.* 2 (119), 210–218. <https://doi.org/10.1289/ehp.1002313>.
- Arnfield, A. John, 2003. Two decades of urban climate research: a review of turbulence, exchanges of energy and water, and the urban heat island. *Int. J. Climatol.* 1 (23), 1–26.
- BD, 2011a. APP-151 Building Design to Foster a Quality and Sustainable Built Environment, Practice Note for Authorized Persons, Registered Structural Engineers and Registered Geotechnical Engineers. Building Department.
- BD, 2011b. APP-152 Sustainable Building Design Guidelines, Practice Note for Authorized Persons, Registered Structural Engineers and Registered Geotechnical Engineers. Buildings Department.
- Besancenot, J.-P., 2002. Heat waves and mortality in large urban areas. *Environ. Risques.* St.(1).
- Bohner, Jürgen, 2006. General climatic controls and topoclimatic variations in Central and high Asia. *Boreas* 2 (35), 279–295. <https://doi.org/10.1111/j.1502-3885.2006.tb01158.x>.
- Böhner, Jürgen, Antonić, Oleg, 2009. Land-surface parameters specific to topo-climatology. *Dev. Soil Sci.* no. 33, 195–226.
- Bottema, Marcel, 1997. Urban roughness modelling in relation to pollutant dispersion. *Atmos. Environ.* 18 (31), 3059–3075. [https://doi.org/10.1016/S1352-2310\(97\)00117-9](https://doi.org/10.1016/S1352-2310(97)00117-9).
- Buscail, Camille, Upegui, Erika, Viel, Jean-François, 2012. Mapping heatwave health risk at the community level for public health action. *Int. J. Health Geogr.* 1 (11), 38. <https://doi.org/10.1186/1476-072x-11-38>.
- Chan, Emily Ying Yang, Goggins, William B., Jakyoung Kim, Jacqueline, Griffiths, Sian M., 2012. A study of intracity variation of temperature-related mortality and socio-economic status among the Chinese population in Hong Kong. *J. Epidemiol. Community Health* 4 (66), 322–327.
- Chan, H.S., Kok, M.H., Lee, T.C., 2012. Temperature trends in Hong Kong from a seasonal perspective. *Clim. Res.* 1 (55), 53–63.
- Chin, P.C., 1986. Climate and weather. In: Chiu, Tse Nang, So, C.L., Catt, P. (Eds.), *A Geography of Hong Kong*. Oxford University Press HK, New York.
- Clarke, John F., 1972. Some effects of the urban structure on heat mortality. *Environ. Res.* 1 (5), 93–104.
- Comrie, Andrew C., 2000. Mapping a wind-modified urban heat island in Tucson, Arizona (with comments on integrating research and undergraduate learning). *Bull. Am. Meteorol. Soc.* 10 (81), 2417–2431. [https://doi.org/10.1175/1520-0477\(2000\)081<2417:mawmu>2.3.co;2](https://doi.org/10.1175/1520-0477(2000)081<2417:mawmu>2.3.co;2).
- DEVB, 2017. Towards a planning vision and strategy transcending 2030 Hong Kong: Development Bureau and Planning Department.
- Dozier, J., Frew, J., 1990. Rapid calculation of terrain parameters for radiation modeling from digital elevation data. *IEEE Trans. Geosci. Remote Sens.* 5 (28), 963–969. <https://doi.org/10.1109/36.58986>.
- Draxler, Roland R., 1986. Simulated and observed influence of the nocturnal urban heat island on the local wind field. *J. Clim. Appl. Meteorol.* 8 (25), 1125–1133. [https://doi.org/10.1175/1520-0450\(1986\)025<1125:saoiot>2.0.co;2](https://doi.org/10.1175/1520-0450(1986)025<1125:saoiot>2.0.co;2).
- Dugord, Pierre-Adrien, Lauf, Steffen, Schuster, Christian, Kleinschmit, Birgit, 2014. Land use patterns, temperature distribution, and potential heat stress risk – the case study Berlin, Germany. *Comput. Environ. Urban Syst.* (48), 86–98. <https://doi.org/10.1016/j.compenvurbsys.2014.07.005>.
- El-Zein, Abbas, Tonmoy, Fahim N., 2015. Assessment of vulnerability to climate change using a multi-criteria outranking approach with application to heat stress in Sydney. *Ecol. Indic.* (48), 207–217. <https://doi.org/10.1016/j.ecolind.2014.08.012>.
- ENB, 2017. *Climate Action Plan 2030+*. Environmental Bureau, Hong Kong.
- Field, Christopher B., 2012. Managing the Risks of Extreme Events and Disasters to Advance Climate Change Adaptation: Special Report of the Intergovernmental Panel on Climate Change. Cambridge University Press.
- Franck, Ulrich, Krüger, Michael, Schwarz, Nina, Grossmann, Katrin, Röder, Stefan, Schlink, Uwe, 2013. Heat stress in urban areas: indoor and outdoor temperatures in different urban structure types and subjectively reported well-being during a heat wave in the city of Leipzig. *Meteorol. Z.* 2 (22), 167–177. <https://doi.org/10.1127/0941-2948/2013/0384>.
- Freund, Rudolf, Jakob, Ramon C., Littell, Creighton, Lee, 2003. Regression using JMP. SAS Institute Inc. and J. Wiley, Cary, NC, USA.
- Gál, T., Unger, J., 2009. Detection of ventilation paths using high-resolution roughness parameter mapping in a large urban area. *Build. Environ.* 1 (44), 198–206.
- Goggins, William B., Chan, Emily Y.Y., Ng, Edward, Ren, Chao, Chen, Liang, 2012a. Effect modification of the association between short-term meteorological factors and mortality by urban heat islands in Hong Kong. *PLoS One* 6 (7), e38551. <https://doi.org/10.1371/journal.pone.0038551>.
- Goggins, William B., Woo, Jean, Ho, Suzanne, Chan, Emily Y.Y., Chau, P.H., 2012b. Weather, season, and daily stroke admissions in Hong Kong. *Int. J. Biometeorol.* 5 (56), 865–872. <https://doi.org/10.1007/s00484-011-0491-9>.
- Hajat, S., Kosatsky, T., 2010. Heat-related mortality: a review and exploration of heterogeneity. *J. Epidemiol. Commun.* H(64). <https://doi.org/10.1136/jech.2009.087999>.
- Hart, Melissa A., Sailor, David J., 2009. Quantifying the influence of land-use and surface characteristics on spatial variability in the urban heat island. *Theor. Appl. Climatol.* 3 (95), 397–406. <https://doi.org/10.1007/s00704-008-0017-5>.
- HKO, 2015. *Monthly Meteorological Normals for Hong Kong, 1981–2010*. Hong Kong Observatory, Hong Kong.
- HKO, 2017a. Extreme weather events in Hong Kong. Hong Kong Observatory, 18 Jan 2018 [cited 23 Jan 2018]. Available from [http://www.hko.gov.hk/climate\\_change/obs\\_hk\\_extreme\\_weather\\_e.htm](http://www.hko.gov.hk/climate_change/obs_hk_extreme_weather_e.htm).
- HKO, 2017b. Summary of Meteorological and Tidal Observations in Hong Kong in 2016. Hong Kong Observatory, Hong Kong.
- Ho, Hung Chak, Ka-Lun Lau, Kevin, Ren, Chao, Ng, Edward, 2017. Characterizing prolonged heat effects on mortality in a sub-tropical high-density city, Hong Kong. *Int. J. Biometeorol.* <https://doi.org/10.1007/s00484-017-1383-4>.
- Hoek, Gerard, Beelen, Rob, Hoogh, Kees de, Vienneau, Danielle, Gulliver, John, Fischer, Paul, Briggs, David, 2008. A review of land-use regression models to assess spatial variation of outdoor air pollution. *Atmos. Environ.* 33 (42), 7561–7578.
- Huang, B., 2017. *Comprehensive Geographic Information Systems*. Elsevier Science.
- IPCC, 2014. *Climate Change 2014–Impacts, Adaptation and Vulnerability: Regional Aspects*. Cambridge University Press, Cambridge, United Kingdom and New York, NY, USA.
- Jennrich, Robert I. 1977. Stepwise regression. Statistical methods for digital computers no. 3, pp. 58–75.
- Kaiser, Reinhard, Tertre, Alain Le, Schwartz, Joel, Gotway, Carol A., Daley, W. Randolph, Rubin, Carol H., 2007. The effect of the 1995 heat wave in Chicago on all-cause and cause-specific mortality (no.). *Am. J. Public Health* 97 (Suppl. 1), S158–S162. <https://doi.org/10.2105/ajph.2006.100081>.
- Ketterer, Christine, Matzarakis, Andreas, 2014. Human-biometeorological assessment of the urban heat island in a city with complex topography – the case of Stuttgart, Germany. *Urban Clim.* 10, 573–584. <https://doi.org/10.1016/j.uclim.2014.01.003>.
- Klein Rosenthal, Joyce, Kinney, Patrick L., Metzger, Kristina B., 2014. Intra-urban vulnerability to heat-related mortality in new York City, 1997–2006. *Health Place* (30), 45–60. <https://doi.org/10.1016/j.healthplace.2014.07.014>.
- Kwan, Mei-Po, 2012. The uncertain geographic context problem. *Ann. Assoc. Am. Geogr.* 5 (102), 958–968. <https://doi.org/10.1080/00045608.2012.687349>.
- Kysely, Jan, 2002. Temporal fluctuations in heat waves at Prague-Klementinum, the Czech Republic, from 1901–97, and their relationships to atmospheric circulation. *Int. J. Climatol.* 1 (22), 33–50. <https://doi.org/10.1002/joc.720>.
- Lai, Edwin S.T., Lee, T.C., Lau, Y.H., 2014. Winds that help a city to breathe. *Bull. Hong. Kong Meteorol. Soc.* (24), 25–32.
- Lam, Hilda, Kok, Mang Hin, Shum, Karen Kit Ying, 2012. Benefits from typhoons – the Hong Kong perspective. *Weather* 1 (67), 16–21. <https://doi.org/10.1002/wea.836>.
- Landsberg, Helmut E., 1981. *The Urban Climate*. Academic press, London.
- Le Tertre, A., Lefranc, A., Eilstein, D., Declercq, C., Medina, S., Blanchard, M., Chardon, B., Fabre, P., Filleul, L., Jusot, J.F., Pascal, L., Prouvost, H., Cassadou, S., Ledrans, M., 2006. Impact of the 2003 heatwave on all-cause mortality in 9 French cities. *Epidemiology*(17). <https://doi.org/10.1097/01.ede.0000187650.36636.1f>.
- Lee, K.L., Chan, Y.H., Lee, T.C., Goggins, William B., Chan, Emily Y.Y., 2016. The development of the Hong Kong heat index for enhancing the heat stress information service of the Hong Kong Observatory. *Int. J. Biometeorol.* 7 (60), 1029–1039. <https://doi.org/10.1007/s00484-015-1094-7>.
- Lemonsu, A., Viguié, V., Daniel, M., Masson, V., 2015. Vulnerability to heat waves: impact of urban expansion scenarios on urban heat island and heat stress in Paris (France). *Urban Clim.* 14, 586–605. <https://doi.org/10.1016/j.uclim.2015.10.007>.
- Leung, Y.K., Yeung, K.H., Ginn, E.W.L., Leung, W.M., 2004. Climate change in Hong Kong. *Hong Kong Obs. Tech. Note*.
- Li, Dan, Bou-Zeid, Elie, 2013. Synergistic interactions between urban heat islands and heat waves: the impact in cities is larger than the sum of its parts. *J. Appl. Meteorol. Climatol.* 9 (52), 2051–2064. <https://doi.org/10.1175/jamc-d-13-021>.
- Macnee, Robert G.D., Tokai, Akihiro, 2016. Heat wave vulnerability and exposure mapping for Osaka City, Japan. *Environ. Syst. Decis.* 4 (36), 368–376. <https://doi.org/10.1007/s10669-016-9607-4>.
- Meehl, Gerald A., Tebaldi, Claudia, 2004. More intense, more frequent, and longer lasting heat waves in the 21st century. *Science* 5686 (305), 994–997.
- Michelozzi, Paola, De’ Donato, Francesca K., Maria Bargagli, Anna, D’Ippoliti, Daniela, De Sario, Manuela, Marino, Claudia, Schifano, Patrizia, Cappai, Giovanna, Leone, Michela, Kirchmayer, Ursula, Ventura, Martina, Gennaro, Marta Di, Leonardi, Marco,

- Oleari, Fabrizio, De Martino, Annamaria, Perucci, Carlo A., 2010. Surveillance of summer mortality and preparedness to reduce the health impact of heat waves in Italy. *Int. J. Environ. Res. Public Health* 5 (7), 2256.
- Miller, A., 2002. *Subset Selection in Regression*. Chapman and Hall/CRC, Boca Raton, FL.
- Miller, Alan J., 1984. Selection of subsets of regression variables. *J. R. Stat. Soc. Ser. A (Gen.)* 3 (147), 389–425. <https://doi.org/10.2307/2981576>.
- Mok, Hing, Yim, Man Chi, Wu, Cheng, Cheuk Yin, 2011. Spatial variation of the characteristics of urban heat island effect in Hong Kong. *J. Civil. Eng. Archit.* 9 (5).
- Ng, Edward, Ren, Chao, 2015. *The urban climatic map: a methodology for sustainable urban planning*. Routledge.
- Ng, Edward, Yuan, Chao, Chen, Liang, Ren, Chao, Fung, Jimmy C.H., 2011. Improving the wind environment in high-density cities by understanding urban morphology and surface roughness: a study in Hong Kong. *Landscape. Urban Plan.* 1 (101), 59–74. <https://doi.org/10.1016/j.landurbplan.2011.01.004>.
- Nunez, Manuel, Oke, Timothy R., 1977. The energy balance of an urban canyon. *J. Appl. Meteorol.* 1 (16), 11–19.
- Oke, T.R., 1973. City size and the urban heat island. *Atmos. Environ.* (1967) 8 (7), 769–779. [https://doi.org/10.1016/0004-6981\(73\)90140-6](https://doi.org/10.1016/0004-6981(73)90140-6).
- Oke, Tim R., 1981. Canyon geometry and the nocturnal urban heat island: comparison of scale model and field observations. *Int. J. Climatol.* 3 (1), 237–254.
- Oke, Tim R., 1988. The urban energy balance. *Prog. Phys. Geogr.* 4 (12), 471–508.
- Oke, Timothy R., 1997. *Urban Environments*. McGill–Queen's University Press.
- Olaya, Victor, 2004. A gentle introduction to SAGA GIS. The SAGA User Group eV, Gottingen, Germany no. 208.
- Peel, Murray C., Finlayson, Brian L., McMahon, Thomas A., 2007. Updated world map of the Köppen-Geiger climate classification. *Hydrol. earth Syst. Sci. Discuss.* 2 (4), 439–473.
- Raupach, M.R., Finnigan, J.J., 1997. The influence of topography on meteorological variables and surface-atmosphere interactions. *J. Hydrol.* 3–4 (190), 182–213. [https://doi.org/10.1016/S0022-1694\(96\)03127-7](https://doi.org/10.1016/S0022-1694(96)03127-7).
- Ryan, Patrick H., LeMasters, Grace K., 2007. A review of land-use regression models for characterizing intraurban air pollution exposure. *Inhal. Toxicol.* s1 (19), 127–133. <https://doi.org/10.1080/08958370701495998>.
- Sall, John, Lehman, Ann, Stephens, Mia L., Creighton, Lee, 2012. *JMP Start Statistics: A Guide to Statistics and Data Analysis Using JMP*. SAS Institute, Cary, NC, USA.
- Sham, Fu-Cheung, 2015. Record-breaking summer temperatures in Hong Kong. *Hong Kong Obs* (19 May 2017 2015)(cited 22 Jun 2017). (Available from). <[http://www.hko.gov.hk/education/article\\_e.htm?title=ele\\_00471](http://www.hko.gov.hk/education/article_e.htm?title=ele_00471)>.
- Shi, Yuan, Katzschnier, Lutz, Ng, Edward, 2018. Modelling the fine-scale spatiotemporal pattern of urban heat island effect using land use regression approach in a megacity. *Sci. Total Environ.* 618, 891–904. <https://doi.org/10.1016/j.scitotenv.2017.08.252>.
- Shi, Yuan, Ka-Lun Lau, Kevin, Ng, Edward, 2017. Incorporating wind availability into land use regression modelling of air quality in mountainous high-density urban environment. *Environ. Res.* (157), 17–29. <https://doi.org/10.1016/j.envres.2017.05.007>.
- Stocker, Thomas, 2014. *Climate Change 2013: The Physical Science Basis: working Group I Contribution to the Fifth Assessment Report of the Intergovernmental Panel on Climate Change*. Cambridge University Press.
- Stone, Brian, Hess, Jeremy J., Frumkin, Howard, 2010. Urban form and extreme heat events: are sprawling cities more vulnerable to climate change than compact cities? *Environ. Health Perspect.* 10 (118), 1425–1428. <https://doi.org/10.1289/ehp.0901879>.
- Su, J.G., Jerrett, M., Beckerman, B., 2009. A distance-decay variable selection strategy for land use regression modeling of ambient air pollution exposures. *Sci. Total Environ.* 12 (407), 3890–3898. <https://doi.org/10.1016/j.scitotenv.2009.01.061>.
- Su, Jason G., Jerrett, Michael, Beckerman, Bernardo, Wilhelm, Michelle, Ghosh, Jo, Kay, Ritz, Beate, 2009. Predicting traffic-related air pollution in Los Angeles using a distance decay regression selection strategy. *Environ. Res.* 6 (109), 657–670. <https://doi.org/10.1016/j.envres.2009.06.001>.
- Svensson, Marie K., 2004. Sky view factor analysis—implications for urban air temperature differences. *Meteorol. Appl.* 03 (11), 201–211.
- Szymanowski, M., Kryza, M., 2009. GIS-based techniques for urban heat island spatialization. *Clim. Res.* 2 (38), 171–187.
- Tabachnick, Barbara G., Fidell, Linda S., 2001. *Using Multivariate Statistics*. Pearson/Allyn & Bacon, Needham Heights, MA, USA.
- Taha, Haider, 1997. Urban climates and heat islands: albedo, evapotranspiration, and anthropogenic heat. *Energy Build.* 2 (25), 99–103. [https://doi.org/10.1016/S0378-7788\(96\)00999-1](https://doi.org/10.1016/S0378-7788(96)00999-1).
- Tan, Jianguo, Zheng, Youfei, Tang, Xu, Guo, Changyi, Li, Liping, Song, Guixiang, Zhen, Xinrong, Yuan, Dong, Kalkstein, Adam J., Li, Furong, Chen, Heng, 2010. The urban heat island and its impact on heat waves and human health in Shanghai. *Int. J. Biometeorol.* 1 (54), 75–84. <https://doi.org/10.1007/s00484-009-0256-x>.
- Tong, Hua, Walton, Andrew, Sang, Jianguo, Chan, Johnny C.L., 2005. Numerical simulation of the urban boundary layer over the complex terrain of Hong Kong. *Atmos. Environ.* 19 (39), 3549–3563. <https://doi.org/10.1016/j.atmosenv.2005.02.045>.
- Tu, Yu-Kang, Kellett, Margaret, Clerehugh, Val, Gilthorpe, Mark S., 2005. Problems of correlations between explanatory variables in multiple regression analyses in the dental literature. *Br. Dent. J.* 7 (199), 457–461.
- Uejio, Christopher K., Wilhelm, Olga V., Golden, Jay S., Mills, David M., Gulino, Sam P., Samenow, Jason P., 2011. Intra-urban societal vulnerability to extreme heat: the role of heat exposure and the built environment, socioeconomics, and neighborhood stability. *Health Place* 2 (17), 498–507. <https://doi.org/10.1016/j.healthplace.2010.12.005>.
- UN, 2016. The New Urban Agenda: Key Commitments. United Nations 2016 [cited 23 Jan 2018]. Available from <<http://www.un.org/sustainabledevelopment/blog/2016/10/newurbanagenda/>>.
- Wang, Weiwen, Zhou, Wen, Ng, Edward Yan Yung, Xu, Yong, 2016. Urban heat islands in Hong Kong: statistical modeling and trend detection. *Nat. Hazards* 2 (83), 885–907. <https://doi.org/10.1007/s11069-016-2353-6>.
- Watson, I.D., Johnson, G.T., 1987. Graphical estimation of sky view-factors in urban environments. *J. Climatol.* 2 (7), 193–197. <https://doi.org/10.1002/joc.3370070210>.
- WHO, 2008. *Improving Public Health Responses to Extreme Weather Heat-Waves EuroHEAT*. World Health Organization Regional Office for Europe, Copenhagen, Denmark.
- Wilby, Robert L., 2007. A review of climate change impacts on the built environment. *Built Environ.* 1 (33), 31–45.
- Wing-lui, Ginn, Tsz-cheung, Lee, Kin-yu, Chan, 2010. Past and future changes in the climate of Hong Kong. *J. Meteorol. Res.* 2 (24), 163–175.
- WMO, WHO, 2015. In: McGregor, Glenn R., Bessemoulin, Pierre, Ebi, Kristie L., Menne, Bettina (Eds.), *Heatwaves and Health: Guidance on Warning-System Development*. World Meteorological Organization.
- Wolf, Tanja, McGregor, Glenn, 2013. The development of a heat wave vulnerability index for London, United Kingdom. *Weather Clim. Extrem.* (1), 59–68. <https://doi.org/10.1016/j.wace.2013.07.004>.
- Wong, M.C., Mok, H.Y., Lee, T.C., 2011. Observed changes in extreme weather indices in Hong Kong. *Int. J. Climatol.* 15 (31), 2300–2311.
- Xie, Dan, Liu, Yi, Chen, Jining, 2011. Mapping urban environmental noise: a land use regression method. *Environ. Sci. Technol.* 17 (45), 7358–7364. <https://doi.org/10.1021/es200785x>.
- Yan, Y.Y., 2007. Surface wind characteristics and variability in Hong Kong. *Weather* 11 (62), 312–316. <https://doi.org/10.1002/wea.46>.
- Yan, Yuk Yee, 2000. The influence of weather on human mortality in Hong Kong. *Soc. Sci. Med.* 3 (50), 419–427. [https://doi.org/10.1016/S0277-9536\(99\)00301-9](https://doi.org/10.1016/S0277-9536(99)00301-9).
- Yang, Xinyan, Li, Yuguo, Luo, Zhiwen, Chan, Pak Wai, 2017. The urban cool island phenomenon in a high-rise high-density city and its mechanisms. *Int. J. Climatol.* 2 (37), 890–904. <https://doi.org/10.1002/joc.4747>.